New divergent dynamics in the isotropic to nematic phase transition of liquid crystals measured with 2D IR vibrational echo spectroscopy

Kathleen P. Sokolowsky, Heather E. Bailey, and Michael D. Fayer[a)]
Department of Chemistry, Stanford University, Stanford, California 94305, USA

(Received 20 August 2014; accepted 24 October 2014; published online 17 November 2014)

The isotropic phase of nematogenic liquid crystals has nanometer length scale domains with pseudonematic ordering. As the isotropic to nematic phase transition temperature (T_{NI}) is approached from above, the orientational correlation length, ξ, of the pseudonematic domains grows as $(T - T^*)^{-1/2}$, where T^* is 0.5–1 K below T_{NI}. The orientational relaxation, which is a collective property of the pseudonematic domains, was measured with optical heterodyne detected-optical Kerr effect (OHD-OKE). The orientational relaxation obeys Landau-de Gennes theory, as has been shown previously. To examine the environmental evolution experienced by molecules in the pseudonematic domains, two-dimensional infrared (2D IR) vibrational echo experiments on the CN stretching mode of the non-perturbative vibrational probes 4-pentyl-4′-selenocyanobiphenyl (5SeCB) and 4-pentyl-4′-thiocyanobiphenyl (5SCB) in the nematogen 4-cyano-4′-pentylbiphenyl (5CB) were performed. The 2D IR experiments measure spectral diffusion, which is caused by structural fluctuations that couple to the CN vibrational frequency. Temperature dependent studies were performed just above T_{NI}, where the correlation length of pseudonematic domains is large and changing rapidly with temperature. These studies were compared to 2D IR experiments on 4-pentylbiphenyl (5B), a non-mesogenic liquid that is very similar in structure to 5CB. The time constants of spectral diffusion in 5CB and 5B are practically identical at temperatures $\geq$5 K above T_{NI}. As the temperature is lowered, spectral diffusion in 5B slows gradually. However, the time constants for spectral diffusion in 5CB slow dramatically and diverge as T^* is approached. This divergence has temperature dependence proportional to $(T - T^*)^{-1/2}$, precisely the same as seen for the correlation length of pseudonematic domains, but different from the observed orientational relaxation times, which are given by the Landau-de Gennes theory. The data and previous results show that spectral diffusion in 5CB has no contributions from orientational relaxation, and the structural dynamics responsible for the spectral diffusion are likely a result of density fluctuations. The results suggest that the correlation length of the density fluctuations is diverging with the same temperature dependence as the pseudonematic domain correlation length, ξ. The isotropic-nematic phase transition in liquid crystals is described in the context of the slowing of orientational relaxation associated with divergent growth of the orientational correlation length. The results presented here show that there is another divergent dynamical process, likely associated with density fluctuations. © *2014 AIP Publishing LLC*. [http://dx.doi.org/10.1063/1.4901081]

I. INTRODUCTION

Here we report observations that reveal fundamentally new structural dynamics in the isotropic phase of liquid crystals as the isotropic to nematic phase transition temperature is approached from above. The results show that there is a dynamic structural property that diverges as the phase transition is approached, and these divergent dynamics are not associated with orientational relaxation. The experiments and calculations strongly suggest that there are density fluctuations that undergo critical slowing down as the phase transition is approached. Therefore, our understanding of the isotropic to nematic phase transition is incomplete, and it is possible that the structure in the nematic phase involves this heretofore unrecognized divergence.

The unique structural, thermodynamic, and optical properties of thermotropic liquid crystals have attracted considerable attention because of the wide variety of liquid crystal applications, ranging from liquid crystal displays, adaptive optical devices for telescopes, solvents for chemical reactions, and optical switchable windows.[1–3] Many of these technologies stem from the ability to manipulate the orientational order within the liquid crystal. A more complete understanding of the fundamental source of liquid crystal structure and dynamics may provide useful insights for future developments and applications.

Nematogens are a variety of liquid crystals that, in the nematic phase, exhibit a degree of net orientational alignment along a direction called the director. At temperatures even tens of degrees above the nematic-isotropic phase transition temperature, T_{NI}, while the liquid is macroscopically isotropic, local orientational order exists, characterized by a correlation length ξ.[4] These regions are referred to as pseudonematic domains. As T_{NI} is approached from above, ξ grows as described by Landau-de Gennes theory until it becomes infinite in the

a)fayer@stanford.edu

nematic phase.[4] The temperature (T) dependence of ξ is given by

$$\xi(T) = \xi_0 \left(\frac{T^*}{T - T^*} \right)^{1/2}, \; T > T^*, \tag{1}$$

where ξ_0 is a molecular length scale (typically 4–8 Å),[5–7] and T^* is the critical temperature normally 0.5–1 K below T_{NI}. In the isotropic phase, the orientational relaxation dynamics are dominated by the complete randomization of the pseudonematic domains.[8–12] When compared to that of normal liquids, the presence of pseudonematic domains results in a significantly different temperature dependence of complete orientational randomization, which is exhibited as the final slow exponential decay of experimentally induced orientational anisotropy. Because of the growing correlation length,[4] the orientational relaxation time, τ_{LdG}, which requires the randomization of the pseudonematic domains, increases and then diverges as T^* is approached from above.[11,13,14] As given by Landau-de Gennes theory,

$$\tau_{LdG} = \frac{V^*_{eff}\eta(T)}{k_B(T - T^*)}, \tag{2}$$

where V^*_{eff} is the nematogen effective volume, $\eta(T)$ is the temperature dependent viscosity, and k_B is the Boltzmann constant.

Numerous techniques including dynamic light scattering[8,10,15,16] and optical heterodyne detected-optical Kerr effect (OHD-OKE) spectroscopy[10,11,13,14,17,18] can measure the orientational relaxation associated with the bulk nematogen liquid in the isotropic phase. To determine the influence of orientational correlation on molecules within a pseudonematic domain, alternate techniques are required. We have previously shown that temperature dependent ultrafast two dimensional infrared (2D IR) vibrational echoes and polarization selective pump-probe experiments combined with the findings from OHD-OKE experiments provide an expanded picture of nematogen dynamics in the isotropic phase.[19,20] The 2D IR experiments yield information on the dynamics experienced by non-perturbative probe molecules within a pseudonematic domain, while the complete reorientation dynamics over a very wide range of time scales are reported by the complementary OHD-OKE experiments.

4-cyano-4′-pentylbiphenyl (5CB) is possibly the most thoroughly examined nematogen partially because of its easily accessible nematic-isotropic phase transition temperature at ∼35 °C.[21] The nitrile stretch of 5CB is a sharp peak at 2230 cm^{-1}.[19,22] Nitrile stretches have previously been shown to be useful vibrational probes for 2D IR experiments, although their utility is frequently limited by the short CN vibrational lifetime.[23–26] 2D IR spectroscopy provides information on structural dynamics through the measurement of spectral diffusion of a vibrational oscillator, like the CN stretch.[27–29] The nitrile absorption band is inhomogeneously broadened because there are a variety of structural environments that shift the vibrational frequency. Spectral diffusion is the time evolution of the vibrational frequencies caused by structural evolution of the liquid. Thus, 2D IR can be used to measure the influence of 5CB pseudonematic domains on the structural dynamics of the liquid.

2D IR spectroscopy of the nitrile stretch of 5CB as the vibrational probe has some substantial experimental pitfalls.[19] The lifetime of the CN stretch is ∼4 ps, which would permit spectral diffusion data to be collected to ∼16 ps under ideal conditions.[19] Large, heat induced peaks caused by vibrational relaxation in the very thin sample (∼3 μm) necessary to study the pure liquid distort the 2D IR spectra by 8 ps. Thus, spectral diffusion measurements on 5CB itself were limited to <8 ps.[19] Difficulties arising from heating were mitigated by examining the carbon-13 nitrile stretch of 5CB, which permitted a thicker sample.[19] However, the short vibrational lifetime (∼8 ps) prevents measurement of complete spectral diffusion, even at the highest temperatures.[19]

To overcome these problems, 5CB was doped with a small amount of 4-pentyl-4′-thiocyanobiphenyl (5SCB). The nitrile stretch of 5SCB has a much longer lifetime, ∼100 ps, than 5CB because of the presence of sulfur, a heavy blocking atom.[19] A thick sample could again be used because of the low concentration of vibrational probe, mitigating deleterious effects caused by heating. Comparisons were made between dynamics reported by the nitrile stretch of 5SCB and the carbon-13 nitrile stretch of 5CB to confirm that the 5SCB reports on the same structural dynamics as an intrinsic probe in neat solution.[19] 2D IR data were collected at four temperatures above T_{NI} for 5SCB in 5CB and for 5SCB in 4-pentylbiphenyl (5B), a structurally similar liquid that is non-mesogenic.[20] We previously found that the time constants of the spectral diffusion were virtually identical in 5CB and 5B at temperatures more than 5 K above T_{NI}, indicating that the presence of pseudonematic domains in 5CB had negligible effect on the structural dynamics reported.[20] However, when the temperature was brought close to T_{NI}, the spectral diffusion in 5CB slowed dramatically to the point that it could not be measured given the lifetime of the CN stretch of 5SCB.[20] An alternate vibrational probe with a longer lifetime was required to probe the effect of pseudonematic domains at temperatures very close to T_{NI}.

Here, we present OHD-OKE, 2D IR vibrational echo, and polarization selective pump-probe data on 2.5 mol% 4-pentyl-4′-selenocyanobiphenyl (5SeCB) in 5CB. We confirm the retention of liquid crystal behavior upon addition of the small amount 5SeCB through comparison of OHD-OKE decays of the doped sample and neat liquid as was done in previous experiments on 5SCB in 5CB.[20] The measured time derivative of the polarizability-polarizability correlation function, which is equivalent to the time derivative of the orientational correlation function (second Legendre correlation function) of the bulk liquid,[30,31] was found to be almost identical between the samples at temperatures above T_{NI}. Landau-de Gennes dynamics for the final exponential relaxation of the pseudonematic domains are preserved, but T^* was ∼1 K lower as compared to the neat sample. The fast, non-exponential portions of the curve are unchanged at all temperatures. Thus, the addition of 5SeCB does not significantly alter the liquid crystal dynamics in 5CB. Most critically, the pseudonematic domains that are fundamental to the isotropic-nematic pretransitional temperature range remain intact.

The heavy blocking atom, Se, between the nitrile stretch and aromatic ring of 5SeCB dramatically increases the vibrational lifetime to ~300 ps in 5CB. To capture the dramatic slowing of the spectral diffusion near T_{NI}, temperature dependent vibrational echo experiments have been conducted on 5SeCB in 5CB at 11 temperatures above T_{NI}; six of them are within 2 K of the phase transition.

Spectral diffusion time constants at temperatures >5 K above T_{NI} were found to be essentially the same in the liquid crystal 5CB and non-mesogenic 5B, within experimental error. The time scale of dynamics begins to differ drastically at temperatures close to T_{NI}. The spectral diffusion in 5B slows, but rather gently, as the temperature is reduced. There is no evidence that suggests a divergence or the existence of any long range order in the non-mesogenic system.

With the ability to measure dynamics to 1 ns, we have quantified the slowing of spectral diffusion close to T_{NI}. At each temperature, the time dependent decay of the spectral diffusion data can be fit to a triexponential. As T_{NI} is approached from above, the three exponential decay times slow dramatically, and show divergent behavior as T^* is approached. The middle and slowest decay time constants are fit very well with a temperature dependence of the form $\alpha[T^*/(T - T^*)]^{1/2}$, which is precisely the same as given by Landau-de Gennes theory for the correlation length of pseudonematic domains, Eq. (1).[4] Even the slowest time constant measured for spectral diffusion, ~1.2 ns, is still orders of magnitude faster than the time required for complete randomization of pseudonematic domains measured by OHD-OKE spectroscopy and given by Eq. (2).[4] The orientational relaxation in 5CB is extremely slow; essentially no significant orientational relaxation occurs on the timescale of the 2D IR experiments. Yet, we observe complete spectral diffusion in hundreds of picoseconds. Thus, orientational fluctuations cannot be the source of spectral diffusion and cannot contribute to the inhomogeneous line broadening in 5CB.

The divergence of the spectral diffusion in the 5CB nematogenic liquid is discussed in the context of critical point phenomena. Theories on the isotropic-nematic transition, including Landau-de Gennes, take orientation as the order parameter for the transition;[4,32–36] the inclusion of density effects in the Landau-de Gennes theory correctly models the transition as weakly first order.[37–39] The orientational correlation length is the distance over which orientational fluctuations are correlated.[4] The orientational properties of liquid crystals have been the subject the bulk of investigations because of their technological significance and the ease with which they can be measured. Here, we propose that density fluctuations are the source of spectral diffusion, which displays the same divergence as T^* is approached as ξ given in Eq. (1). The results suggest that there is a density correlation length that diverges as T^* is approached. Divergence in the correlation length of density fluctuations as the temperature approaches T_c is known for supercritical fluids.[40] It is possible that there is a growing density correlation length and a critical slowing down of density fluctuations that may be associated with the isotropic to nematic transition critical phenomena.

II. EXPERIMENTAL PROCEDURES

A. Sample preparation

5B and 5CB were purchased from TCI America and Sigma Aldrich, respectively. 5SCB was synthesized as described previously.[19] 5SeCB was synthesized in a two-step procedure from 4-bromo-4′-pentylbiphenyl. The aryl bromide was converted to 4-amino-4′-pentylbiphenyl as previously published.[19] The resulting aryl amine was diazotized and reacted with potassium selenocyanate as suggested by McCulla to yield 5SeCB.[41] The crude brown product was purified with a silica column to give a yellow solid with a total yield of ~40%. The identity and purity of the solid were verified by ^{1}H and ^{13}C NMR, FT-IR, and mass spectrometry. Details of the synthesis and product characterization are given in the supplementary material.[42]

Solutions of 2.5 mol% 5SCB in 5B and 2.5 mol% 5SeCB in 5CB were each passed through a 0.02 μm filter (Anotop) before loading in to the appropriate sample cell. For OHD-OKE experiments, the 5SeCB in 5CB sample was contained between two 3 mm thick CaF_2 windows held at 1 cm path length in a custom cell. For FT-IR and ultrafast infrared experiments, solutions were sandwiched between two 3 mm thick CaF_2 windows, separated by a 390 μm Teflon spacer, contained in a copper sample cell. The sample cell temperature was varied from approximately 300–350 K and maintained at each temperature with a PID temperature controller to ±0.1 K.

B. Optical heterodyne detected-optical Kerr effect spectroscopy

The OHD-OKE experiment is a nonresonant spectroscopic technique in which a linearly polarized pump pulse induces a transient birefringence in a sample. The time decay of the birefringence (related to the orientational relaxation) is measured by a physically delayed probe pulse, polarized at 45° relative to the pump. Birefringence induced by the pump pulse causes a ellipticity in the probe pulse that is measured after a crossed polarizer.[43,44] The signal decays with time as the birefringence is reduced by orientational relaxation. The signal is the derivative of the polarizability-polarizability correlation function, which is the same as the derivative of the orientational relaxation correlation function (second Legendre polynomial correlation function) at all but very short times where interaction induced (collision induced) contributions may influence the signal.[30,31]

The details of the OHD-OKE setup have been described in detail previously.[45] Briefly, a Ti:Sapphire oscillator/regenerative amplifier produces pulses at 5 kHz repetition rate with energy up to 300 μJ/pulse and pulse widths that are varied from 60 fs to 125 ps depending on the time scale being studied. Because of the nonresonant nature of this experiment, the pulses can be chirped to change their duration without affecting the measured dynamics. The regen output is beam split into the pump and probe beams.

The signal is heterodyned to improve the signal to noise and to permit a phase cycling pulse sequence. The data are taken with a four shot sequence in which the phase of

the probe heterodyne field and the pump polarization are cycled.[45,46] Data are obtained with a balanced detector and a lock-in amplifier. Data can be collected from hundreds of femtoseconds to microseconds. For the data taken at long time, the probe pulse and delay line are replaced with a CW probe beam, and a 1 ns digitizer is employed to record the data.

OHD-OKE data were collected for 2.5 mol% 5SeCB in 5CB. Each decay was fit using the phenomenological function,

$$F(t) = [pt^{-z} + dt^{b-1}]e^{-t/\tau}, \tag{3}$$

which has been used to fit OHD-OKE data for many liquids including liquid crystals[17,47,48] and is based on schematic mode coupling theory.[49–51] The power laws describe the early time non-Markovian caged dynamics prior to a final exponential decay, which is the complete orientational randomization. For the nematogen 5CB, this final decay is the Landau-de Gennes decay, which is the pseudonematic domain randomization.[17] For this paper, we are primarily interested in the exponential. However, to obtain an accurate fit, a global fit of the entire data must be performed because the power laws influence the analysis of the exponential decay.

Data were fit from 1 ps to near the end of the exponential. The endpoint of the fit varied from 2.9×10^5 ps for samples at 309.7 K to 7.5×10^3 ps at 349.2 K. Like previous experiments, the exponents of the power laws were found to be temperature independent.[17,18,20] The data were fit again holding these parameters constant at their average, and the quality of the fits did not change, but the number of adjustable parameters and the error bars on the exponential decay times were reduced.

C. FT-IR spectroscopy

FT-IR spectra were collected with a resolution of 1 cm^{-1}. The nitrile absorption peak of 5SeCB is at 2154 cm^{-1} in 5CB. The peak is slightly temperature dependent, experiencing a red-shift of less than half a wave number as the temperature is increased by 40 K over the range of interest. Background subtraction of neat 5CB at corresponding temperatures was performed to isolate the 5SeCB nitrile band for data analysis.

D. Ultrafast infrared spectroscopy

The methods and experimental setup for ultrafast experiments have been described in detail in previous publications and are briefly summarized below.[29,52] A Ti:Sapphire oscillator/regenerative amplifier pumped an optical parametric amplifier (OPA) to generate ~6 μJ pulses of mid-IR light. These pulses were approximately 150 fs in duration at 1 kHz repetition rate. The center wavelength of the IR was tuned to 2158 cm^{-1} and had a spectrum of ~90 cm^{-1} full width at half maximum. The OPA output was then split in to two beams for pump-probe spectroscopy and four beams for vibrational echo spectroscopy. The timing of pulse arrival at the sample was set with delay lines, which provide a maximum experimental window of ~2 ns.

For pump-probe experiments, the generated mid-IR light is divided in to a weak probe pulse and a much stronger pump pulse, which are crossed in the sample. The polarization of the pump pulse is rotated relative to the probe to selectively extract information on the population relaxation and orientational dynamics of the sample. The decay of the probe transmission was collected with the pump polarizations parallel ($I_\parallel$) and at the magic angle (I_{ma}) relative to the probe; these decays are given by

$$\begin{aligned} I_\parallel &= P(t)(1 + 0.8C_2(t)), \\ I_{ma} &= P(t), \end{aligned} \tag{4}$$

where $P(t)$ is the vibrational population relaxation and $C_2(t)$ is the second Legendre polynomial correlation function (orientational correlation function). Measuring both polarizations permits the extraction of $C_2(t)$ from measurements of $I_\parallel$ if the timescale of the orientational relaxation is not significantly slower than the vibrational population relaxation of the probe.

The probe (signal) was dispersed in a spectrograph and detected by a mercury-cadmium-telluride 32 element array detector. Analysis of the vibrational lifetime of the nitrile stretch of 5SeCB was complicated by the fact that both the 0-1 and 1-2 transitions are overlapped by the much stronger 1-2 transition of the carbon-13 nitrile stretch of 5CB. The desired information can be obtained by fitting the population decay to a biexponential holding one of the decay times equal to that obtained from the fit to the vibrational lifetime of the ^{13}CN stretch found from a neat sample.[19] Because the ^{13}CN lifetime is so much shorter than the SeCN lifetime, it only affects the short time portion of the decay.

In vibrational echo experiments, three excitation pulses are crossed in the sample. A much weaker fourth pulse serves as a local oscillator (LO). The time between pulses 1 and 2 is the coherence time, τ; the time between pulses 2 and 3 is the population time, T_w. Nonlinear interactions of the three excitations pulses give rise to a fourth pulse, the vibrational echo, at a time $\leq\tau$ after the third excitation pulse. The echo propagates in a unique direction. The LO is then spatially and temporally overlapped with the vibrational echo. This heterodyne detection amplifies the vibrational echo and provides phase information through the temporal interference between the LO and echo pulses. At a given T_w, data were collected by scanning τ; this causes the vibrational echo pulse to move in time relative to the temporally fixed LO pulse. The resulting temporal interferogram was frequency resolved and detected on the 32-element array, providing the vertical axis, ω_m, of the 2D IR spectra. At each ω_m the interferogram is numerically Fourier transformed to give the horizontal axis, ω_τ, of the 2D IR spectra. Data were collected at T_w's ranging from 0.5 ps to 1 ns.

The change in shape of the 2D IR spectrum of the nitrile stretch of 5SCB and 5SeCB as a function of T_w is caused by spectral diffusion, which reports on the structural dynamics of 5B and 5CB. A range of CN transition frequencies exists, giving rise to inhomogeneous broadening of the nitrile absorption band. The liquid structure interacting with an individual nitrile stretch determines the center frequency of its narrow Lorentzian line produced by homogeneous broadening. The total absorption line is the collection of all individual

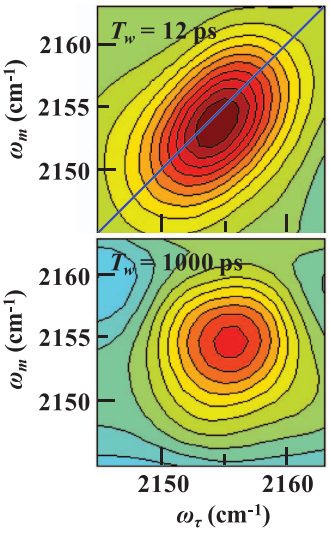

FIG. 1. 2D IR spectra of the nitrile stretch of 2.5 mol% 5SeCB in 5CB at 306.9 K. At the short $T_w = 12$ ps, the 0-1 transition is elongated along the diagonal. When $T_w = 1000$ ps, the spectrum becomes closer to round. Information on spectral diffusion is contained in the change in shape of the spectrum with time.

molecules' Lorentzians with a Gaussian distribution of center frequencies. Structural fluctuations of the medium, either 5B or 5CB here, cause changes in frequency of the nitrile probe. Thus, the frequency of a particular molecule will evolve in time as the liquid structure changes (spectral diffusion). At sufficiently long T_w, the vibrational probe will have sampled all liquid structures, hence all of the frequencies present in the inhomogeneously broadened FT-IR absorption spectrum.

In effect, the first and second pulses of the vibrational echo pulse sequence "label" the initial probe frequencies. Then during the waiting time, T_w, between pulse 2 and 3, the structure of the liquid evolves, causing the nitrile frequencies to shift. This period is ended by the arrival of the third pulse, which also stimulates the emission of the vibrational echo pulse. The echo contains information on the final frequencies of the vibrational oscillators. When T_w is short, the structure of the liquid is relatively unchanged from when the vibrations were first labeled, producing final frequencies that differ little from the starting frequencies. At longer T_w, the liquid structure has more time to evolve, and the final frequencies are less correlated with the initial frequencies. The loss of correlation as T_w increases is manifested as a change in shape of the 2D IR spectrum. As an example, two 2D IR spectra taken on the CN stretch of 5SeCB in 5CB at 306.9 K are shown in Figure 1.

At early times, the detection frequency (ω_m) is correlated with the starting frequency (ω_τ), producing a spectrum that is elongated along the diagonal (top panel Figure 1). As T_w increases and frequencies are less correlated, the shape of the spectrum becomes more symmetrical. When the population time is long enough for all of the environments to be sampled, the spectrum will become round. The bottom panel of Figure 1 displays data at long time when spectral diffusion is almost complete, and the spectrum is almost round. Thus, the structural dynamics of the liquid can be extracted from the change in shape of the 2D IR spectra as a function of T_w.

The amplitudes and timescales of spectral diffusion are quantified by the frequency-frequency correlation function (FFCF). The FFCF is the joint probability that a vibrational oscillator with an initial frequency will have that same frequency at a later time, averaged over all of the initial frequencies in the inhomogeneous spectral distribution. The Center Line Slope (CLS) method[53,54] is used to extract the FFCF from the T_w dependence of the shape of the 2D IR spectra.

The FFCF was modeled with the form

$$C(t) = \langle \delta\omega(\tau_1)\delta\omega(0)\rangle = \sum_i \Delta_i^2 \exp(-t/\tau_i), \qquad (5)$$

where Δ_i and τ_i are the frequency fluctuation amplitude and time constant, respectively, of the i^{th} component. A component of the FFCF is motionally narrowed and a source of homogeneous broadening in the absorption line if $\Delta\tau < 1$. In this instance, it is not possible to determine Δ and τ individually. The motionally narrowed contribution to the absorption spectrum has a pure dephasing line width given by $\Gamma^* = \Delta^2\tau = 1/\pi T_2^*$, where T_2^* is the pure dephasing time. The homogeneous time that is measured, T_2, also depends on the orientational relaxation and vibrational lifetime, given by

$$\frac{1}{T_2} = \frac{1}{T_2^*} + \frac{1}{2T_1} + \frac{1}{3T_{or}}, \qquad (6)$$

where T_1 and T_{or} are the vibrational lifetime and orientational relaxation time. The CLS has been previously shown to be mathematically equivalent to the normalized T_w-dependent portion of the FFCF.[53,54] Combining the T_w dependence from the CLS with the linear absorption spectrum of the vibrational probe enables the homogeneous contribution to be determined.[53,54] The resulting full FFCF is obtained.[53,54]

III. RESULTS AND DISCUSSION

A. OHD-OKE results

OHD-OKE decays of 2.5 mol% 5SeCB in 5CB were collected over a range of temperatures above the nematic-isotropic phase transition. Figure 2 shows data at three temperatures. The data have been offset for clarity. They span many decades in time and amplitude. As with neat 5CB and 5CB with 5SCB, each of these decays can be fit with Eq. (3).[17,18,20,51] The values of the power law exponents for the 5SeCB doped 5CB sample are the same as those obtained for neat 5CB and 5CB containing 5SCB within experimental error. This is not surprising as 5SeCB is structurally very similar to 5SCB, which was shown to have no effect on the short time dynamics within experimental error. In addition to fitting the data with the phenomenological function in Eq. (3), modified schematic mode coupling theory (MCT) for the isotropic phase of liquid crystals can be used to fit the data to give detailed information on the orientational and density correlation functions.[18,20] The red dashed line through the 328 K data is the fit using MCT. The relationship between the MCT fits and the 2D IR experiments is discussed in detail below in Sec. III D 3.

With the addition of viscosity data, a Landau-de Gennes plot for the 5SeCB in 5CB sample was constructed. From

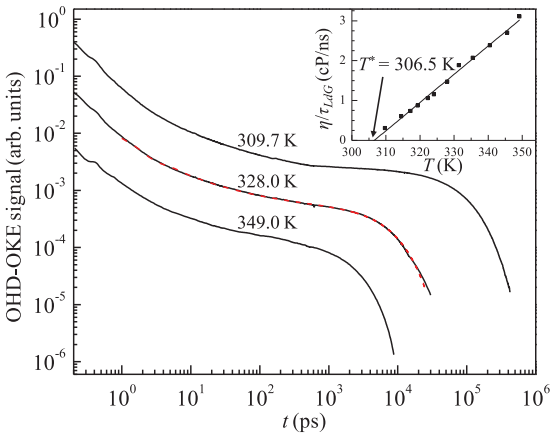

FIG. 2. Temperature-dependent 5CB with 2.5 mol% 5SeCB OHD-OKE data at three temperatures. The curves have been offset along the vertical axis for clarity. Each decay was fit with the function given by Eq. (3). The red dashed line is the fit from modified schematic MCT.[20] The inset shows a Landau-de Gennes plot from the results for the long time exponential decay and viscosity data. The x-intercept of the linear fit gives $T^* = 306.5$ K for the doped sample of 5CB.

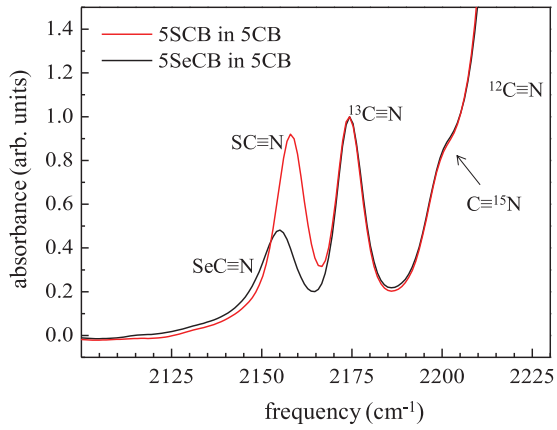

FIG. 3. Normalized FT-IR spectrum of 2.5 mol% 5SCB in 5CB and 2.5 mol% 5SeCB in 5CB, both at 329.0 K. The CN stretch of 5SCB is at 2157 cm^{-1} and ~8.5 cm^{-1} FWHM. The CN stretch of 5SeCB is at 2154 cm^{-1} and ~9.5 cm^{-1} FWHM. Both of these peaks slightly overlap with the ^{13}CN stretch of 5CB, but the resulting 2D IR signals can be readily resolved.

Eq. (2), it can be seen that a plot of η/τ_{LdG} versus temperature should be linear with the x-intercept giving T^*. As shown in the inset of Figure 2, the 5SeCB doped 5CB sample obeys Landau-de Gennes theory. The x-intercept is 306.5 K, approximately one degree lower than that of pure 5CB. The critical temperature found for the 5SeCB doped sample is higher than that of 5SCB in 5CB, previously found to be 303.8 K.[20] Improved sample quality is the likely source of the smaller temperature depression from T^* of neat 5CB. Small amounts of impurities have been shown to have significant effect on the nematic-isotropic phase transition temperature of 5CB.[55,56]

Agreement between the power laws of the OHD-OKE decays is evidence that the presence of 5SeCB does not significantly perturb the dynamics within the pseudonematic domains. The correlation lengths of the domains themselves are equivalent to those in neat 5CB 1 K higher temperature. Thus, as with 5SCB, measurements of the spectral diffusion of the 5SeCB probe in 5CB are performed on a sample that has the liquid crystal properties of the 5CB nematogen.

B. Linear infrared spectroscopy

The nitrile stretch absorption of 5SeCB in CCl_4 is located at ~2158 cm^{-1}. This is in agreement with center frequency of the nitrile stretch of phenyl selenocyanate in the neat liquid.[57–59] When dissolved at 2.5 mol% in 5CB, the nitrile stretch of 5SeCB was found to absorb at 2154 cm^{-1}. As can be seen in Figure 3, the nitrile absorption of 5SeCB overlaps with the red tails of the carbon-12 and carbon-13 nitrile stretches of 5CB, but the 2D IR signal can still be readily separated (see below). Although present at approximately 2.5 times the concentration of the carbon-13 nitrile stretch of 5CB, the nitrile absorption of 5SeCB has a significantly lower optical density because it has a smaller transition dipole.

As observed with the nitrile stretches of 5CB and 5SCB in 5CB,[19] the center frequency of the nitrile stretch of 5SeCB is slightly temperature dependent. As the temperature is increased from just above to T_{NI} to approximately 40 K above T_{NI}, the peak center shifts to the red by ~0.5 cm^{-1}. A very slight broadening with increased temperature is also observed.

C. Polarization selective pump-probe spectroscopy

Magic angle and parallel geometry pump-probe experiments were performed on the nitrile stretch of 5SeCB in 5CB at four temperatures spanning a range up to 40 degrees above T_{NI}. The lifetime was found to be 305 ± 5 ps, independent of temperature over the range examined. This value is consistent with previous work that found the lifetime of the nitrile stretch of phenyl selenocyanate to be ~282 ps in CCl_4 solution.[59] The exceedingly long lifetime of the nitrile stretch of 5SeCB relative to other vibrational probes typically used for ultrafast infrared experiments dramatically increases the experimental window for pump-probe and spectral diffusion measurements to 1 ns.

As was measured previously for vibrational probes in the isotropic phase of 5CB, the magic angle and parallel pump-probe decays of 5SeCB in 5CB were found to be identical at each temperature.[19,20] The identical decays for the two measurements demonstrate that the time scale of the orientational relaxation, $C_2(t)$, is substantially slower than the population relaxation. The population relaxation time is ~300 ps. Therefore, the orientational relaxation time is greater than several nanoseconds. Orientational relaxation was previously observed in the non-mesogenic liquid 5B using the 5SCB probe.[20] As $C_2(t)$ decays negligibly in 5CB, orientational relaxation cannot be a source of the spectral diffusion observed in the 2D IR experiments.

D. Vibrational echo spectroscopy

1. 5SCB in 5B

To explicate the dynamics due to the presence of pseudonematic domains in 5CB, we need to fully characterize the spectral diffusion in the non-mesogenic liquid 5B. 5B has

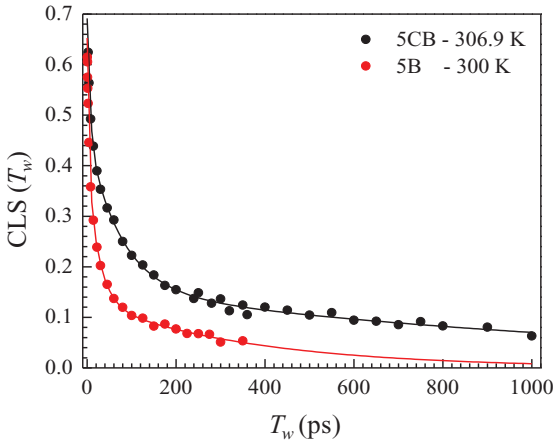

FIG. 4. 2D IR CLS data (points) for 2.5 mol% 5SCB in 5B (red) at 300 K and 2.5 mol% 5SeCB in 5CB (black) at 306.9 K. Both curves are fit to triexponential decays with no offset (solid curves). The quality of data and fit is similar at all other temperatures. The resulting FFCF parameters for all temperatures are given in Table I for 5SCB in 5B and Table II for 5SeCB in 5CB.

a very similar molecular structure to 5CB, and we previously found the spectral diffusion time constants of 5SCB in 5B to match those in 5CB at temperatures well above the phase transition temperature.[20] At 305.5 K, which is approaching the phase transition in 5CB, the spectral diffusion in 5B did not show the same dramatic slowing that was observed in the nematogen.[20]

A more complete picture of the temperature dependence of liquid structural evolution in a normal liquid was obtained by collecting 2D IR data at three additional temperatures: 300, 320, and 340 K. At the coldest temperature, 300 K, the 2D IR spectrum is essentially round (complete spectral diffusion) at 400 ps.

An example CLS obtained from 2D IR spectra of 5SCB in 5B (red circles) and the fit (red solid curve) are shown in Figure 4. At this temperature and all of the other temperatures, the data can be fit well to a triexponential decay. The FFCF parameters for the fits at all temperatures can be found in Table I. As the temperature is lowered from 349 K to 300 K, all of the time constants increase. The short and middle time constants increase from 1.5 to 3.5 ps and 5 to 25 ps, respectively, as the sample temperature is decreased by 50 K. The important point is that the temperature dependence is mild. The long time constant (τ_{long}) obtained from the triexponential fit of 5SCB in 5B spectral diffusion data ranges from roughly 80 to 350 ps as the temperature is lowered. Like the shorter time constants, τ_{long} only increases by a factor of ~4.5. The mild temperature dependence of the 5B spectral diffusion is consistent with the fact that 5B is a "normal" liquid, lacking the liquid crystal isotropic to nematic phase transition and the pseudonematic domains that grow in correlation length as the temperature is lowered toward T^*.

2. 5SeCB in 5CB

When the 5SeCB in 5CB sample temperature was held significantly above T_{NI}, the spectral diffusion time constants were the same as those obtained for 5SCB in 5B within experimental error. The data did not indicate the presence of pseudonematic domains. However, when the temperature was set relatively close to T^*, the spectral diffusion dynamics were shown to slow significantly compared to those in 5B.[20] The experimental window at the time was limited to 180 ps and it was not possible to quantify the dynamics as $T - T^*$ approached zero. The synthesis of the longer lived vibrational probe 5SeCB permitted spectral diffusion to be measured very close to T^*.

T_{NI} was found to be 306.8 K, which is slightly higher than the 5SCB doped 5CB likely because of improved overall sample purity. Initially, spectral diffusion data were acquired for 5SeCB in 5CB out to 200 ps at 310, 329 and 349 K for comparison to previous work with the 5SCB probe. Within experimental error, the dynamics reported by the nitrile stretch of 5SeCB are indistinguishable from those reported by the nitrile stretch of 5SCB. The CLS data for both 2.5 mol% 5SCB and 5SeCB in 5CB at 329 K are shown in Figure 5; the solid red curve is a triexponential fit to the combined data. Thus, the 5SeCB probe reports on the same liquid structural evolution as carbon-13 nitrile in 5CB by transitivity.[20] Combined with the results from OHD-OKE, we can confidently probe the effect of pseudonematic domains in 5CB with the nitrile stretch of 5SeCB.

We focused the bulk of our 2D IR experiments just above the nematic-isotropic phase transition temperature. Data at six temperatures (306.9, 307.2, 307.5, 307.8, 308.1, and 308.5 K) were taken within two degrees of T_{NI}; the coldest is just 0.1 K above the transition temperature. It is here, exceedingly close

TABLE I. FFCF parameters for 2.5 mol% 5SCB in 5B.[a]

T (K)	Δ_1 (cm^{-1})	τ_1 (ps)	Δ_2 (cm^{-1})	τ_2 (ps)	Δ_3 (cm^{-1})	τ_3 (ps)	Γ (cm^{-1})	T_2 (ps)
349.0	1.4 ± 0.2	1.5 ± 1.5	1.9 ± 0.2	5.4 ± 1.8	1.3 ± 0.2	75 ± 4	3.4 ± 0.3	3.1 ± 0.3
340.0	1.7 ± 0.2	2.4 ± 0.8	1.6 ± 0.2	11 ± 3	1.2 ± 0.2	109 ± 10	3.5 ± 0.3	3.0 ± 0.3
329.0	1.6 ± 0.2	2.5 ± 1.3	1.6 ± 0.2	12 ± 4	1.3 ± 0.2	121 ± 16	3.4 ± 0.3	3.1 ± 0.3
320.0	1.8 ± 0.2	3.6 ± 0.3	1.7 ± 0.2	18 ± 2	1.2 ± 0.2	179 ± 11	3.2 ± 0.3	3.4 ± 0.3
310.0	1.8 ± 0.2	3.2 ± 0.9	1.7 ± 0.2	26 ± 6	1.2 ± 0.2	191 ± 29	3.1 ± 0.3	3.5 ± 0.3
305.5	1.8 ± 0.2	3.1 ± 0.6	1.9 ± 0.2	21 ± 2	1.3 ± 0.2	296 ± 22	2.6 ± 0.3	4.1 ± 0.4
300.0	1.7 ± 0.2	3.5 ± 0.6	1.9 ± 0.2	25 ± 3	1.3 ± 0.2	360 ± 30	2.8 ± 0.3	3.9 ± 0.4

[a]The Δ_i are the standard deviations of the i^{th} component of the inhomogeneous contribution to the absorption line. The standard deviation of the total inhomogeneous linewidth is $(\Sigma_i \Delta_i^2)^{1/2}$. The full width at half maximum (FWHM) of the inhomogeneous component of the absorption line is 2.35 times the standard deviation of the total inhomogeneous component. The FWHM of the total absorption spectrum is the convolution of the FWHM of the homogeneous linewidth, Γ, with the FWHM of the inhomogeneous component. The total absorption line shape is a Voigt profile.

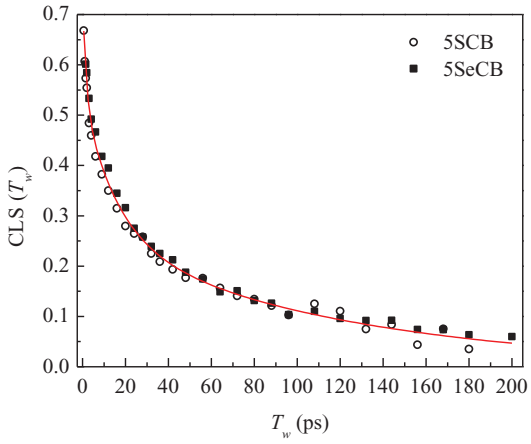

FIG. 5. 2D IR CLS data (points) for 2.5 mol% 5SCB (open circles) and 2.5 mol% 5SeCB (closed squares) in 5CB at 329 K. A triexponential fit to the combined data is shown as a solid line. Within experimental error, the nitrile stretches of 5SCB and 5SeCB report on the same structural dynamics. After 200 ps, the spectral diffusion in 5CB at 329 K is essentially complete.

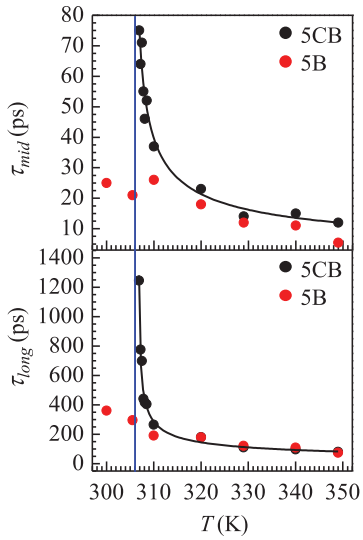

FIG. 6. Middle (top) and long (bottom) time constants from the triexponential fits for spectral diffusion in 5CB (black) and 5B (red) as a function of temperature. The vertical blue line is located at $T^* = 306.5$ K found from OHD-OKE spectroscopy. The time constants of spectral diffusion in 5CB are fit to the functional form $A|T\text{-}x|^p$. A divergent slowing down in the dynamics of 5CB is observed at T^*.

to T_{NI}, where the effect from pseudonematic domains should be the largest. The correlation length of pseudonematic domains is proportional to $(T - T^*)^{-1/2}$,[4] so it will change significantly over the 2 K just above T_{NI}. We cannot get closer to T^* because of the weakly first order nature of the transition. In addition to these six temperatures, we also collected 2D IR data at five temperatures spanning 310–349 K to obtain a more complete picture of the temperature dependence.

The CLS of the coldest temperature, 306.9 K, is shown in Figure 4 (black circles). When the temperature of the sample was held above 310 K, the measured spectral diffusion was complete within the first few hundred picoseconds. At the coldest temperature, spectral diffusion is not complete even at 1 ns as can be seen in Figure 4 where the data have decayed to ~0.06 but have not yet reached zero.

At all temperatures, the CLS decay of the nitrile stretch of 5SeCB in 5CB can be fit to a triexponential. The solid black curve in Figure 4 is the triexponential fit to the 306.9 K data. The FFCF parameters for these fits are in Table II. As in 5B, we see all of the decay constants increase as the temperature is lowered. But unlike the spectral diffusion time constants in 5B, the time constants in 5CB increase dramatically as the temperatures is lowered by just tenths of a degree near T_{NI}. The error in the shortest time constant is fairly significant relative to the value of the time constant because of the data acquisition start time of $T_w = 1.5$ ps. The fastest decay constant increases substantially at low temperatures, but we will focus further discussion on the middle (τ_{mid}) and long time constant (τ_{long}), which have smaller error bars.

Figure 6 shows the temperature dependence of τ_{mid} and τ_{long} for both 5SCB in 5B and 5SeCB in 5CB. The vertical blue line is the value of T^*found from OHD-OKE experiments. At >310 K, the time constants for the two liquids are essentially identical. This agrees with our previous work, where no difference was observed between the spectral diffusion in a nematogen and a non-mesogenic liquid at higher temperatures.[20] Now, we are able to quantify the dramatic slowing as T^* is approached. Both of the 5CB spectral diffusion time constants, τ_{mid} and τ_{long}, deviate drastically from those obtained for 5B. The spectral diffusion in 5CB diverges as T^* is approached. It is only close to T^* that the presence of pseudonematic domains affects the spectral diffusion in 5CB.

TABLE II. FFCF parameters for 2.5 mol% 5SeCB in 5CB.

T (K)	Δ_1 (cm^{-1})	τ_1 (ps)	Δ_2 (cm^{-1})	τ_2 (ps)	Δ_3 (cm^{-1})	τ_3 (ps)	Γ (cm^{-1})	T_2 (ps)
349.0	2.2 ± 0.2	1.1 ± 1.3	2.7 ± 0.2	12 ± 2	1.8 ± 0.2	81 ± 7	3.3 ± 0.3	3.2 ± 0.3
340.0	1.4 ± 0.3	1.1 ± 0.3	2.6 ± 0.2	15 ± 3	1.8 ± 0.2	97 ± 11	4.2 ± 0.4	2.5 ± 0.4
329.0	1.8 ± 0.2	1.0 ± 1.2	2.4 ± 0.2	14 ± 4	2.3 ± 0.2	111 ± 7	3.3 ± 0.3	3.2 ± 0.3
320.0	1.9 ± 0.2	2.7 ± 1.4	2.2 ± 0.2	23 ± 7	2.2 ± 0.2	181 ± 18	3.4 ± 0.3	3.1 ± 0.3
310.0	2.0 ± 0.2	3.9 ± 1.0	2.1 ± 0.2	37 ± 7	2.2 ± 0.2	265 ± 19	3.5 ± 0.3	3.0 ± 0.3
308.5	2.2 ± 0.2	2.2 ± 0.6	2.2 ± 0.2	52 ± 9	1.9 ± 0.2	405 ± 35	3.6 ± 0.3	2.9 ± 0.3
308.1	2.1 ± 0.2	5.5 ± 1.7	2.1 ± 0.2	46 ± 12	2.2 ± 0.2	417 ± 33	3.0 ± 0.3	3.5 ± 0.3
307.8	2.2 ± 0.2	4.8 ± 1.2	2.1 ± 0.2	55 ± 12	2.1 ± 0.2	441 ± 38	3.1 ± 0.3	3.4 ± 0.3
307.5	2.2 ± 0.2	4.8 ± 0.8	2.3 ± 0.2	71 ± 8	1.8 ± 0.2	699 ± 59	3.0 ± 0.3	3.5 ± 0.3
307.2	2.2 ± 0.2	5.4 ± 1.1	2.3 ± 0.2	64 ± 8	1.9 ± 0.2	776 ± 64	3.1 ± 0.3	3.5 ± 0.3
306.9	2.0 ± 0.2	7.6 ± 1.5	2.4 ± 0.2	75 ± 7	1.7 ± 0.2	1250 ± 130	3.4 ± 0.3	3.1 ± 0.3

TABLE III. Temperature dependence of CLS time constants.

	A (ps)	x (K)	p
τ_{short}	4.6 ± 0.9	306.6 ± 0.3	0.39 ± 0.11
τ_{mid}	85 ± 18	305.6 ± 0.5	0.52 ± 0.06
τ_{long}	502 ± 32	306.7 ± 0.1	0.48 ± 0.03

The temperature dependence of τ_{mid} and τ_{long} for 5SeCB in 5CB can be fit to the functional form $\tau = A|T - x|^p$. The resulting fit parameters can be found in Table III, and the fits (solid curves) are shown in Figure 6. Within experimental error, $x = T^*$ for both the middle and long time constants. So not only are the time constants rapidly increasing as the phase transition is approached from above, but they are diverging at T^*. This is characteristic of critical phenomena. Additionally, the fits to both τ_{mid} and τ_{long} have $p = -1/2$ within experimental uncertainty. We can then rewrite the functions that fit that data as

$$\tau_{mid} = \alpha_{mid}\left(\frac{T^*}{T - T^*}\right)^{1/2} \quad \text{and}$$

$$\tau_{long} = \alpha_{long}\left(\frac{T^*}{T - T^*}\right)^{1/2}, \quad T > T^*. \tag{7}$$

α_{mid} and α_{long} are scaling constants with $\alpha_{mid} = 4.9$ (ps) and $\alpha_{long} = 29$ (ps). This is the same functional form as Eq. (1), which gives the correlation length of the pseudonematic domains as a function of temperature.

The direct proportionality of τ_{mid} and τ_{long} with ξ is shown in Figure 7. ξ has been calculated using Eq. (1) taking $\xi_0 = 4$ Å.[5–7] The pseudonematic domain correlation length and time constants for spectral diffusion are well correlated. The net result is that the spectral diffusion undergoes critical slowing down as T^* is approached from above and the divergence tracks the growth of the correlation length of the pseudonematic domains. This divergence is very different from that displayed by the orientational relaxation. Orientational relaxation is influenced by the presence of pseudonematic domains many tens of degrees above T^*. In addition, the orientational relaxation diverges as T^* is approached as given in Eq. (2), that is, as $(T - T^*)^{-1}$ rather than as given in Eq. (7), where the exponent is −1/2. Because of this difference, the spectral diffusion in the isotropic phase behaves the same as a normal liquid until the temperature is within a few degrees of T^*. Then the question is what type of structural fluctuations are responsible for the spectral diffusion and its divergence as T^* is approached from above.

3. The nature of spectral diffusion

Spectral diffusion is produced by fluctuations of the environment that cause the transition frequencies of the vibrational probes to evolve through the frequencies of the inhomogeneously broadened absorption line.[27–29] From analysis of OHD-OKE data using modified schematic MCT that was adapted to deal with the isotropic phase of liquid crystals,[18] we know that the orientational correlation decays negligibly on the timescale of the 2D IR experiment.[18,20] Figure 8 shows

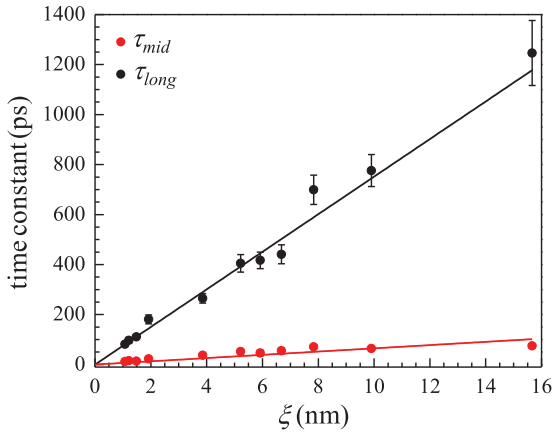

FIG. 7. Middle (red) and long (black) time constants from the triexponential fits for spectral diffusion in 5CB as a function of correlation length. The correlation lengths were calculated via Eq. (1) with $\xi_0 = 4$ Å and $T^* = 306.7$ K (the value of x found from the fit of t_{long} vs. T). The divergent spectral diffusion dynamics in 5CB show the same temperature dependence as ξ. Linear fits to decay constant versus ξ are shown.

the 5CB orientational correlation function (a) and the density correlation function (b) obtained from the fit to the OHD-OKE data at 328 K. The MCT fit to the experimental data is shown in Figure 2. As can be seen in Figure 8(a), the orientational correlation function decays negligibly, ∼4%, over the first 250 ps. The inset shows that at 25 ns the orientational correlation function has not completely decayed to zero, even at this relatively high temperature compared to T^*. It is important to note again that the OHD-OKE data are the derivative of the orientational correlation function. Therefore, the orientational correlation function obtained from the MCT fit is accurate as its derivative reproduces the experimental data almost perfectly. In addition, the polarization selective pump-probe experiments show that there is no orientational relaxation on the time scale of the spectral diffusion. Therefore, a second observable demonstrates that the time scale for orientational relaxation is extremely slow. This is in sharp contrast to the spectral diffusion, which at 329 K has decayed almost to zero by 200 ps (see Figure 5). Close to T^*, spectral diffusion approaches zero in ∼1 ns (see Figure 4), but the orientational correlation function decays on the microsecond time scale.

The OHD-OKE data and the MCT analysis show that orientational fluctuations are much too slow to contribute to spectral diffusion in 5CB. Additionally, complete decay of the CLS to zero (complete spectral diffusion) instead of a constant value at long time demonstrates that there is no very slow component of the spectral diffusion. At 329 K, all structures that contribute to the inhomogeneous line have been sampled in several hundred picoseconds. Even at 306.9 K, spectral diffusion is complete in several nanoseconds rather than the microseconds required for complete orientational relaxation. These results demonstrate that orientational relaxation does not play a role in the spectral diffusion. In addition, because spectral diffusion is complete without contributions from orientational relaxation, the inhomogeneous broadening of the CN stretch absorption line of 5SeCB does not have contributions from orientational disorder.

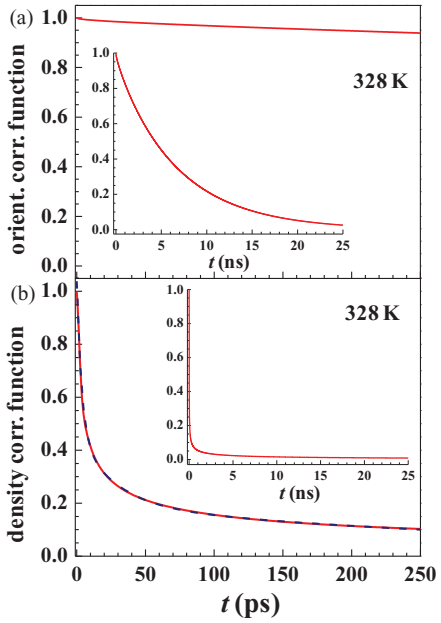

FIG. 8. Plots of the orientational correlation function (a) and the density correlation function (b) for 5CB doped with 2.5 mol% 5SeCB obtained from an MCT fit to the OHD-OKE data at 328 K. The OHD-OKE data and corresponding MCT fit are shown in Figure 2. The time axes for the main figures are in picoseconds while the insets are in nanoseconds. The density correlation function is fit with a triexponential decay, shown as the dashed blue line.

In addition to the inhomogeneous broadening contribution to the absorption spectrum, there is also the homogeneous (Lorentzian) component. Homogeneous broadening is produced by ultrafast motions that result in motional narrowing. The homogeneous broadening component is obtained from the full CLS analysis. The homogeneous linewidths are given in Tables I and II. While orientational relaxation does not contribute to spectral diffusion, fast librational motions can contribute to the homogeneous broadening of the absorption line. Librations, which are orientational oscillations of a molecule, occur on a sub-picosecond time scale. Neutron scattering studies suggest that there are sub-picosecond motions around the long axis of 5CB.[60] Such ultrafast motions give rise to the homogeneous linewidth but not to the spectral diffusion and its divergence as T^* is approached. While librations are too fast to contribute to the observed spectral diffusion, orientational relaxation is much too slow.

Once orientational fluctuations have been eliminated as the source of spectral diffusion, translational and density fluctuations remain as the possible causes of inhomogeneous broadening of the absorption spectrum and of spectral diffusion in 5CB. Self-diffusion studies by NMR have been performed by a number of groups.[61–64] In the isotropic phase, Dvinskikh and Furo report Arrhenius-type behavior with an activation energy of ~33 kJ/mol.[61] Slightly above T_{NI}, the isotropic self-diffusion constant was found to be approximately 5.3×10^{-10} m^2/s, roughly 1 ns to diffuse 1 Å. They present no evidence to suggest a divergence in translational fluctuations as the isotropic-nematic transition is approached from above.

Figure 8(b) shows the density correlation function obtained from the MCT fit (red curve) and a triexponential fit to it (dashed blue curve).[20] By 250 ps, the density correlation function has decayed close to zero. The density correlation function decays on approximately the same time scale as the spectral diffusion (compare Figures 8(b) and 5). The triexponential fit to the density correlation function yields time constants within a factor of 2 or 3 of the spectral diffusion time constants. However, the schematic MCT assumes that the important density fluctuations are short-range.[65,66] It is not designed to capture a growing correlation length of density fluctuations.[18,20] The important point to be taken away from the MCT analysis is that, as shown by both the OHD-OKE data and the MCT analysis, orientational relaxation is far too slow to contribute to the observed spectral diffusion. However, the MCT analysis shows that the decay of the density correlation function is on the same time scale as the spectral diffusion (CLS decay). These results suggest that density fluctuations are responsible for the spectral diffusion and its divergence as T^* is approached.

We can gain some insights by examining static and dynamic critical point phenomena. The divergence of static parameters as a critical point is approached are described by critical exponents.[67,68] For instance, the correlation length divergence in the disordered phase is proportional to $(T - T_c)^{-\nu}$. Using mean field Ginzburg-Landau theory, $\nu = \frac{1}{2}$.[67] This agrees with the typical definition for orientational correlation length of pseudonematic domains in liquid crystals. The slowing down of dynamics near a critical point is defined in relation to the growing correlation length.[69] The relaxation rate τ is proportional to $\xi(T)^z = (T - T_c)^{-\nu z}$, where typically $z \geq 1$.[67] Our result that the time constants of spectral diffusion diverge as $(T - T^*)^{-1/2}$ corresponds to $z = 1$. Thus, it is not unreasonable to assign the slowing down of spectral diffusion to a diverging correlation length of density fluctuations as T^* is approached from above. For super critical fluids, Saitow *et al.* report an analogous phenomena for the correlation length and density fluctuations for non-hydrogen bonded fluids above the critical point.[40] While the isotropic to nematic phase transition is not the same as a gas-liquid critical point, both the isotropic liquid crystal and supercritical fluid experience drastic pretransitional effects due to a growing correlation length.

IV. CONCLUDING REMARKS

Ultrafast infrared spectroscopy and optical heterodyne detected-optical Kerr effect experiments were used to elucidate the influence of pseudonematic domains on the structural dynamics in the isotropic phase of the liquid crystal 5CB. 2D IR and polarization selective pump-probe experiments were conducted on a dilute vibrational probe, 5SeCB, which has a long vibrational lifetime. OHD-OKE spectroscopy was utilized to confirm that the addition of the probe molecule did not disturb the liquid crystal nature of the nematogen and to obtain the orientational and density correlation functions using schematic MCT. The orientational relaxation is dominated by the randomization of pseudonematic domains; these domains are characterized by a length ξ, the distance over which the

nematogens' orientations are correlated. As T_{NI} is approached from above, ξ grows proportional to $(T - T^*)^{-1/2}$.

The results presented above show that the spectral diffusion in 5CB measured by 2D IR is strongly influenced by proximity to T_{NI}. By comparison, the structurally similar, nonmesogenic liquid 5B displays normal liquid dynamics that change mildly with temperature. We have found that the temperature dependence of the time constants for spectral diffusion in 5CB, as given by Eq. (7), is precisely the same as that of the pseudonematic domain correlation length, ξ, given in Eq. (1). As demonstrated here, although the spectral diffusion diverges as ξ diverges, orientational fluctuations do not contribute to the spectral diffusion.[20] The orientational relaxation in 5CB is far too slow compared to the observed spectral diffusion to contribute. Additionally, the time for complete orientational randomization of pseudonematic domains is proportional to $\eta/(T - T^*)$, a significantly more severe temperature dependence than observed for the temperature dependence of spectral diffusion. The results suggest that density fluctuations are the likely source of spectral diffusion in 5CB, and that the correlation length of these fluctuations diverges as T^* is approached from above. Theories of critical points contain the $(T - T_c)^{-1/2}$ divergence of the correlation length of fluctuations as a starting point from which the divergence of other parameters, such as C_v or κ_T, are derived.[70] The slowing down of dynamics upon approaching a critical point has been noted to diverge as $\xi(T)^z$, where z is typically ≥ 1. Our finding of $z = 1$ for the slowing down of spectral diffusion as the isotropic-nematic transition is approached from above is in accord with the general theory of critical points.

ACKNOWLEDGMENTS

This work was funded by the Division of Chemistry, Directorate of Mathematical and Physical Sciences, National Science Foundation Grant No. CHE-1157772. K.P.S. thanks Stanford for a Graduate Research Fellowship.

[1] I. C. Sage, in *Handbook of Liquid Crystals*, edited by D. Demus, J. Goodby, G. W. Gray, H.-W. Spiess, and V. Vill (Wiley-VCH Verlag GmbH, 1998), Vol. 1, p. 731.
[2] W. A. Crossland and T. D. Wilkinson, in *Handbook of Liquid Crystals*, edited by D. Demus, J. Goodby, G. W. Gray, H.-W. Spiess, and V. Vill (Wiley-VCH Verlag GmbH, 1998), Vol. 1, p. 763.
[3] W. J. Leigh and M. S. Workentin, in *Handbook of Liquid Crystals*, edited by D. Demus, J. Goodby, G. W. Gray, H.-W. Spiess, and V. Vill (Wiley-VCH Verlag GmbH, 1998), Vol. 1, p. 839.
[4] P. G. deGennes and J. Prost, *The Physics of Liquid Crystals* (Clarendon Press, 1974).
[5] A. Sinha, T. A. Prasada Rao, and R. Dabrowski, J. Phys. Soc. Jpn. **68**, 1939 (1999).
[6] G. Carbone and R. Barberi, Phys. Rev. E **71**, 051704 (2005).
[7] J. J. Krich, M. B. Romanowsky, and P. J. Collings, Phys. Rev. E **71**, 051712 (2005).
[8] T. D. Gierke and W. H. Flygare, J. Chem. Phys. **61**, 2231 (1974).
[9] E. G. Hanson, Y. R. Shen, and G. K. L. Wong, Phys. Rev. A **14**, 1281 (1976).
[10] J. D. Litster, J. Appl. Phys. **41**, 996 (1970).
[11] J. J. Stankus, R. Torre, C. D. Marshall, S. R. Greenfield, A. Sengupta, A. Tokmakoff, and M. D. Fayer, Chem. Phys. Lett. **194**, 213 (1992).
[12] T. W. Stinson and J. D. Litster, Phys. Rev. Lett. **30**, 688 (1973).
[13] S. D. Gottke, H. Cang, B. Bagchi, and M. D. Fayer, J. Chem. Phys. **116**, 6339 (2002).
[14] H. Cang, J. Li, and M. D. Fayer, Chem. Phys. Lett. **366**, 82 (2002).
[15] P. Stepanek and B. Sadlacek, J. Polym. Sci., Polym. Symp. **61**, 123 (1977).
[16] M. R. Dodge, R. G. Petschek, and C. Rosenblatt, Phys. Rev. E **68**, 031703 (2003).
[17] H. Cang, J. Li, V. N. Novikov, and M. D. Fayer, J. Chem. Phys. **119**, 10421 (2003).
[18] J. Li, H. Cang, H. C. Anderson, and M. D. Fayer, J. Chem. Phys. **124**, 014902 (2006).
[19] K. P. Sokolowsky and M. D. Fayer, J. Phys. Chem. B **117**, 15060 (2013).
[20] K. P. Sokolowsky, H. E. Bailey, and M. D. Fayer, J. Phys. Chem. B **118**, 7856 (2014).
[21] G. W. Gray, K. J. Harrison, and J. A. Nash, Electron. Lett. **9**, 130 (1973).
[22] L. M. Babkov, I. I. Gnatyuk, G. A. Puchkovskaya, and S. V. Trukhachev, J. Struct. Chem. **43**, 1019 (2002).
[23] J. K. Chung, M. C. Thielges, S. J. Bowman, K. L. Bren, and M. D. Fayer, J. Am. Chem. Soc. **133**, 6681 (2011).
[24] J. K. Chung, M. C. Thielges, and M. D. Fayer, Proc. Natl. Acad. Sci. U.S.A. **108**, 3578 (2011).
[25] Y. S. Kim and R. M. Hochstrasser, J. Phys. Chem. B **113**, 8231 (2009).
[26] S. Bagchi, S. G. Boxer, and M. D. Fayer, J. Phys. Chem. B **116**, 4034 (2012).
[27] S. Mukamel, Annu. Rev. Phys. Chem. **51**, 691 (2000).
[28] S. Mukamel, *Principles of Nonlinear Optical Spectroscopy* (Oxford University Press, New York, 1995).
[29] S. Park, K. Kwak, and M. D. Fayer, Laser Phys. Lett. **4**, 704 (2007).
[30] D. McMorrow and W. T. Lotshaw, J. Chem. Phys. **95**, 10395 (1991).
[31] D. McMorrow, W. T. Lotshaw, and G. A. Kenney-Wallace, IEEE J. Quantum Electron. **24**, 443 (1988).
[32] S. Singh, Phys. Rep. **324**, 107 (2000).
[33] P. G. de Gennes, Mol. Cryst. Liq. Cryst. **12**, 193 (1971).
[34] L. Onsager, Ann. N.Y. Acad. Sci. **51**, 627 (1949).
[35] W. Maier and A. Saupe, Z. Naturforsch. **14a**, 882 (1959).
[36] W. Maier and A. Saupe, Z. Naturforsch. **15a**, 287 (1960).
[37] P. K. Mukherjee, T. R. Bose, D. Ghose, and M. Saha, Phys. Rev. E: Stat. Phys., Plasmas, Fluids **51**, 4570 (1995).
[38] P. K. Mukherjee, Mod. Phys. Lett. B **11**, 107 (1997).
[39] B. Nandi, P. K. Mukherjee, and M. Saha, Mod. Phys. Lett. B **10**, 777 (1996).
[40] K.-I. Saitow, D. Kajiya, and K. Nishikawa, J. Phys. Chem. A **109**, 83 (2005).
[41] R. D. McCulla and W. S. Jenks, J. Am. Chem. Soc. **126**, 16058 (2004).
[42] See supplementary material at http://dx.doi.org/10.1063/1.4901081 for synthetic procedures and characterization of 4-pentyl-4′-selenocyanobiphenyl.
[43] N. A. Smith and S. R. Meech, Int. Rev. Phys. Chem. **21**, 75 (2002).
[44] S. Kinoshita, Y. Sakai, J. Miyazaki, and J. Watanabe, Eur. Phys. J.: Spec. Top. **209**, 1 (2012).
[45] A. L. Sturlaugson, K. S. Fruchey, and M. D. Fayer, J. Phys. Chem. B **116**, 1777 (2012).
[46] A. L. Sturlaugson, A. Y. Arima, H. E. Bailey, and M. D. Fayer, J. Phys. Chem. B **117**, 14775 (2013).
[47] B. G. Nicolau, A. Sturlaugson, K. Fruchey, M. C. C. Ribeiro, and M. D. Fayer, J. Phys. Chem. B **114**, 8350 (2010).
[48] A. L. Sturlaugson, K. S. Fruchey, S. R. Lynch, S. R. Aragon, and M. D. Fayer, J. Phys. Chem. B **114**, 5350 (2010).
[49] H. Cang, J. Li, and M. D. Fayer, J. Chem. Phys. **119**, 13017 (2003).
[50] H. Cang, V. N. Novikov, and M. D. Fayer, J. Chem. Phys. **118**, 2800 (2003).
[51] H. Cang, J. Li, V. N. Novikov, and M. D. Fayer, J. Chem. Phys. **118**, 9303 (2003).
[52] J. Zheng, K. Kwak, and M. D. Fayer, Acc. Chem. Res. **40**, 75 (2007).
[53] K. Kwak, S. Park, I. J. Finkelstein, and M. D. Fayer, J. Chem. Phys. **127**, 124503 (2007).
[54] K. Kwak, D. E. Rosenfeld, and M. D. Fayer, J. Chem. Phys. **128**, 204505 (2008).
[55] R. R. Reddy, A. Venkatesulu, K. Rama Gopal, and K. N. Reddy, J. Mol. Liq. **130**, 112 (2007).
[56] G. A. Oweimreen, A. K. Shihab, K. Halhouli, and S. F. Sikander, Mol. Cryst. Liq. Cryst. **138**, 327 (1986).
[57] S. Giorgianni, A. Passerini, and R. Passerini, Spectrosc. Lett. **16**, 775 (1983).
[58] E. E. Aynsley, N. N. Greenwood, and M. J. Sprague, J. Chem. Soc. **1965**, 2395.
[59] H. Bian, J. Li, X. Wen, and J. Zheng, J. Chem. Phys. **132**, 184505 (2010).
[60] H. Suzuki, A. Inaba, J. Krawczyk, M. Massalska-Arodz, T. Kikuchi, and O. Yamamuro, J. Non-Cryst. Solids **357**, 734 (2011).

[61]S. V. Dvinskikh and I. Furo, J. Chem. Phys. **115**, 1946 (2001).
[62]R. Y. Dong, J. Chem. Phys. **88**, 3962 (1988).
[63]P. Holstein, M. Bender, P. Galvosas, D. Geschke, and J. Karger, J. Magn. Reson. **143**, 427 (2000).
[64]R. Blinc, B. Marin, J. Pirs, and J. W. Doane, Phys. Rev. Lett. **54**, 438 (1995).
[65]L. Sjögren, Phys. Rev. A **33**, 1254 (1986).
[66]W. Götze and L. Sjögren, Transp. Theory Stat. Phys. **24**, 801 (1995).
[67]U. C. Tauber, Lect. Notes Phys. **716**, 295 (2007).
[68]J. Cardy, *Scaling and Renormalization in Statistical Physics* (Cambridge University Press, Cambridge, 1996).
[69]P. C. Hohenberg and B. I. Halperin, Rev. Mod. Phys. **49**, 435 (1977).
[70]D. Chandler and I. Oppenheim, J. Chem. Phys. **49**, 2121 (1968).